

# PARAMETRIC STUDY OF MICROPILLAR ARRAY SOLAR CELLS

Heayoung P. Yoon<sup>1</sup>, Yu A. Yuwen<sup>1</sup>, Haoting Shen<sup>2</sup>, Nikolas J. Podraza<sup>1</sup>, Thomas E. Mallouk<sup>3</sup>, Elizabeth C. Dickey<sup>2</sup>, Joan A. Redwing<sup>2</sup>, Christopher R. Wronski<sup>1</sup>, and Theresa S. Mayer<sup>1</sup>

<sup>1</sup>Department of Electrical Engineering, The Pennsylvania State University, University Park, PA, USA

<sup>2</sup>Department of Materials Science and Engineering, The Pennsylvania State University, University Park, PA, USA

<sup>3</sup>Department of Chemistry, The Pennsylvania State University, University Park, PA, USA

## ABSTRACT

Micro/nano pillar arrays can be a promising architecture for high efficiency solar cells based on less expensive photovoltaic materials with short minority carrier diffusion lengths ( $L_{n,p}$ ). To investigate design tradeoffs of the radial junction array solar cells, we fabricated 25  $\mu\text{m}$ -tall *c*-Si pillar array devices having different diameters and pillar filling ratio. The high-aspect-ratio radial  $p^+n^+$  junctions were formed by gas phase diffusion of an n-type dopant into etched p-type Si pillars. The *c*-Si pillar arrays showed clear rectifying properties. The spectral reflectance decreased with the pillar filling ratio increase from 0.2 to 0.5, but no subsequent decrease was observed above the filling ratio of 0.5. On the other hand, approximately two times higher cell efficiency was obtained with an 8  $\mu\text{m}$  diameter ( $<1 L_n$ ) pillar array than with a 32  $\mu\text{m}$  diameter ( $>3 L_n$ ) pillar array having the same pillar filling ratio.

## INTRODUCTION

High-aspect-ratio micro/nanopillar arrays are a promising geometry for high efficiency solar cells based on less expensive photovoltaic (PV) materials, where higher impurity levels and crystalline defects lead to a reduction in the minority carrier diffusion length ( $L_{n,p}$ ) [1]. Unlike planar cells, where light absorption and carrier collection are in competition, the alternative geometry of radial *p-n* junction pillars offers the advantage of decoupling of the processes [2]. The three dimensional cells can be thick in the direction of incident light to maximize the absorption of solar radiation, while at the same time thin in the direction of carrier collection to facilitate the efficient extraction of light-generated carriers. Recent studies have demonstrated significant potential of radial junction pillar array solar cells with different types of active materials including vertically aligned VLS grown Si nanowires [3], etched Si micropillars [4] [5], and CdS/CdTe core/shell nanopillars [6]. As proposed in theoretical calculations [7][8], the radial junction array cell performances can significantly depend on the cell geometric configurations, yet a few experimental studies has been provided. Here, we fabricated densely-packed *c*-Si pillar array solar cells having different diameters ( $1L_n - 3L_n$ ) and filling ratio (FR; 0.2 – 0.6). The pillar array cells were characterized by dark and light current-voltage (*I-V*) measurements as well as their spectral response measurements. The direct and

quantitative comparison of these cells offers important insight for the design tradeoffs of radial junction pillar array solar cells that are made using emerging low-cost materials and processes.

## EXPERIMENTAL

Hexagonally packed pillar arrays were etched in a *p*-type single crystalline (100) silicon substrate (*c*-Si). The resistivity of the double-side polished substrate was 0.02 – 0.03  $\Omega\cdot\text{cm}$ , corresponding to doping concentrations of  $5\times 10^{18} \text{ cm}^{-3}$ . While the height of the pillars is approximately equal to the optical thickness of the *c*-Si material ( $\approx 25 \mu\text{m}$ ) for all cells, the diameter and filling fraction of the pillars vary systematically from  $1L_n$  to  $3L_n$  and 0.2 to 0.6, respectively.

As illustrated in Figure 1, the pillar array cells were fabricated using deep reactive ion etching (DRIE) process with a  $\text{SiO}_2$  hard mask. The process cycles between sulfur hexafluoride ( $\text{SF}_6$ ) gas etching ( $5\times 10^{-6} \text{ m}^3/\text{s}$  (300 sccm), 3.5 s) and octafluorocyclobutane ( $\text{C}_4\text{F}_8$ ) polymer deposition ( $5\times 10^{-6} \text{ m}^3/\text{s}$  (300 sccm), 1s) under a pressure of 4 Pa (30 mTorr) and power of 1500 W at 20 °C, providing a Si etch rate of 2.5  $\mu\text{m}/\text{min}$ . The sidewall roughness and damage introduced during DRIE were significantly reduced by incorporating oxygen plasma cleaning ( $3.3\times 10^{-6} \text{ m}^3/\text{s}$  (200 sccm), 4 Pa (30 mTorr), 1800 W, 5 min), Piranha cleaning ( $\text{H}_2\text{SO}_4:\text{H}_2\text{O}_2=1:1$ ), and two successive thermal oxidation and strip cycles prior to dopant diffusion. Radial junctions ( $n^+p^+$ ) were formed by gas phase diffusion (1000 °C, 13 min) from phosphorus oxychloride ( $\text{POCl}_3$ ), giving a surface doping concentration of  $\approx 10^{20} \text{ cm}^{-3}$  and a junction depth of  $\approx 0.3 \mu\text{m}$ . The minority carrier diffusion length is approximately 10  $\mu\text{m}$  for the heavily doped p-type Si ( $5\times 10^{18} \text{ cm}^{-3}$ ) and 0.2  $\mu\text{m}$  for the n-type Si ( $10^{20} \text{ cm}^{-3}$ ) [9]. Al/p-Si contacts were formed by thermal evaporation (300 nm thick) onto the backside of the devices and annealing at 600 °C for 10 minutes in nitrogen ( $\text{N}_2$ ) atmosphere. A layer of Ti(50nm)/Au(100 nm) was deposited on the n-type Si following a native oxide removal in buffered oxide etchant (BOE 1:50, 30 s), serving as top contacts.

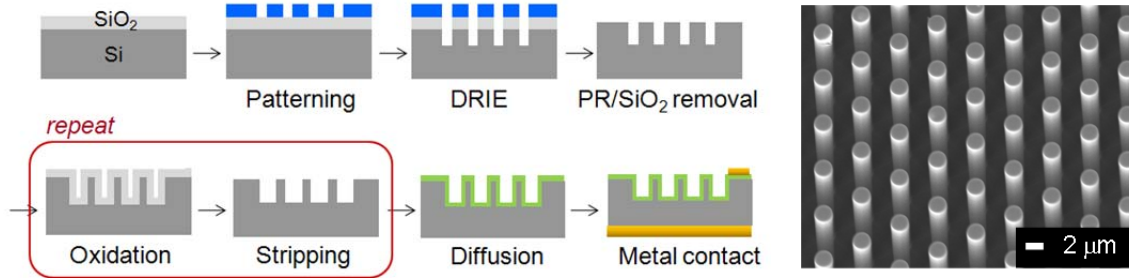


**Figure 1** Fabrication procedure for hexagonally-packed etched pillar array solar cells. A SEM image (right) shows a portion of the device.

Figure 1(right) shows a field emission scanning electron microscope image of a small portion etched pillar array device. A typical active cell area is  $3.3 \text{ mm} \times 3.3 \text{ mm}$ , where a  $2.5 \text{ mm} \times 2.5 \text{ mm}$  pillar array was surrounded by a  $0.4 \text{ mm}$  wide planar junction. The dark the light  $I$ - $V$ s were measured using a semiconductor analyzer and a solar simulator with an Air Mass 1.5G source. For a reflectance measurement, we used a large area ( $5 \text{ mm} \times 5 \text{ mm}$ ) pillar arrays that were fabricated under identical conditions. The reflectance spectra were obtained using a UV-Vis-NIR spectrophotometer with the integration sphere diffuse reflectance attachment.

## RESULTS AND DISCUSSION

The fabricated  $c$ -Si pillar array solar cells showed clear rectifying properties with an ideality factor ( $n$ ) of 1.2 to 1.6. The saturation current density ( $J_0$ ) of the pillar array cells is about two orders of magnitude higher than that of planar control cells ( $n=1.1$ ,  $J_0=3.3 \text{ pA/cm}^2$ ) that were processed under identical conditions. The lower electrical quality of  $n^+$ - $p^+$  junctions in the pillar array devices is probably caused by residual sidewall damage introduced in the DRIE process. We compared the light  $I$ - $V$  characteristics of the etched pillar arrays having different filling ratio of pillars and different diameters, respectively.

### (1) Variable: filling ratio

Figure 2 shows the spectral reflectance of the different filling ratio of pillars in devices in a wavelength ( $\lambda$ ) range of 350–850nm. While all devices were designed to have  $8 \mu\text{m}$  diameter and  $25 \mu\text{m}$  tall pillars, the distances between the pillars are  $16 \mu\text{m}$ ,  $9 \mu\text{m}$ ,  $6 \mu\text{m}$ ,  $4 \mu\text{m}$ ,  $3 \mu\text{m}$ , and  $2 \mu\text{m}$  for the corresponding filling ratio of 0.2, 0.3, 0.4, 0.5, and 0.6, respectively. The variation of diameter and height of the fully fabricated pillars was  $\approx 0.5 \mu\text{m}$ . The reflectance decreased linearly with the pillar filling ratio increase from 0.2 to 0.5 and no decrease above  $\text{FR}=0.5$  saturating at values  $\approx 40\%$  below that of a bare Si.

$I$ - $V$  curves are shown in Fig.3, and table 1 provides a summary of the PV characteristics. The reflectance of the  $\text{FR}=0.2$  cell is  $\approx 7\%$  higher than that of the  $\text{FR}=0.5$  cell,

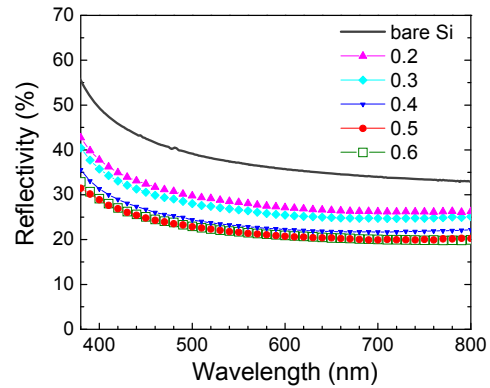


**Figure 2** Reflectance spectra of devices with pillar arrays ( $25 \mu\text{m}$  tall,  $8 \mu\text{m}$  diameter) but having different pillar filling ratio of the devices

possibly accounting for  $\approx 7\%$  reduction of short-circuit current density,  $J_{sc}$  ( $\approx 1.4 \text{ mA/cm}^2$ ). However, the obtained  $J_{sc}$  with the  $\text{FR}=0.2$  and  $\text{FR}=0.5$  cell was  $13.3 \text{ mA/cm}^2$  and  $20 \text{ mA/cm}^2$ , respectively (Table 2). The significantly low  $J_{sc}$  in the  $\text{FR}=0.2$  cell implies that the additional enhancement of the  $J_{sc}$  due to the multiple reflections within the pillars and between adjacent pillars is quite small. Our previous work suggested that a large enhancement would occur due to a ledge around the base of the pillars ( $\approx 30^\circ$ ) in the case of  $\text{FR}=0.5$  cell [4].

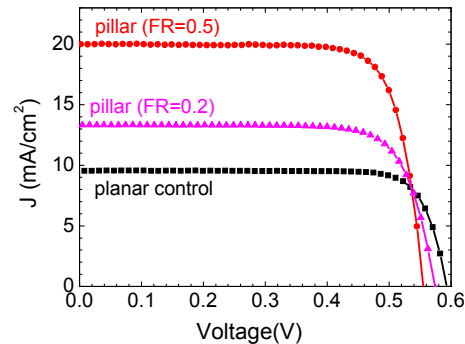


**Figure 3** Light  $J$ - $V$  characteristics of planar and  $\text{FR}=0.2$  and  $\text{FR}=0.5$  pillar array

**Table 1 Photovoltaic performance under AM 1.5G illumination of FR=0.2 and FR=0.5 pillar arrays (25  $\mu\text{m}$  tall, 8  $\mu\text{m}$  diameter)**

	n	$J_{\text{dark}}$ (A/cm <sup>2</sup> )	$J_{\text{sc}}$ (mA/cm <sup>2</sup> )	$V_{\text{oc}}$ (V)	FF (%)	efficiency (%)
planar	1.1	$3.3 \times 10^{-12}$	9.6	0.592	80.8	4.6
FR 0.2	1.4	$9.7 \times 10^{-10}$	13.3	0.573	77.3	5.8
FR 0.5	1.5	$9.2 \times 10^{-10}$	20.0	0.555	78.1	8.7

## (2) Variable: diameter

Figure 4 shows the properties of pillar arrays with diameters of 8  $\mu\text{m}$  ( $\approx 1L_n$ ) and 32  $\mu\text{m}$  ( $\approx 3L_n$ ). Both devices maintain the same filling ratio (FR=0.5) and the height of the pillars (25  $\mu\text{m}$ ). To achieve the filling ratio of 0.5, the designed distances between the pillars are 3  $\mu\text{m}$  and 11  $\mu\text{m}$  for the pillar diameters of 8  $\mu\text{m}$  and 32  $\mu\text{m}$ , respectively.

The photovoltaic parameters of the two pillar arrays are listed in Table 2. The significantly lower  $J_{\text{sc}}$  of the 32  $\mu\text{m}$  diameter pillar array ( $\approx 11 \text{ mA/cm}^2$ ) than that of the 8  $\mu\text{m}$  diameter pillar array solar cell (20  $\text{mA/cm}^2$ ) is mainly due to the loss of photo-generated carriers by recombination in the pillars. The value of  $J_{\text{sc}}$  of the 32  $\mu\text{m}$  diameter pillar array is close to that of the planar control cell (9.6  $\text{mA/cm}^2$ ). Although the open-circuit voltage ( $V_{\text{oc}}$ ; 0.573 V) is slightly higher than that of 8  $\mu\text{m}$  diameter pillar array (0.555 V), the overall power conversion efficiency of the 32  $\mu\text{m}$  diameter pillar array ( $\eta=4.8\%$ ) is  $\approx 2X$  smaller than that of  $\mu\text{m}$  diameter pillar array ( $\eta=8.7\%$ ).

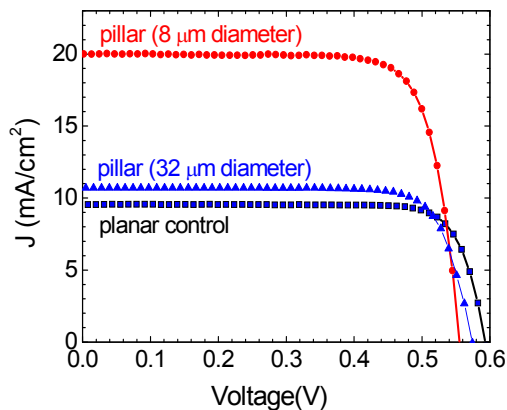


**Figure 4 Light J-V characteristics of planar, 8  $\mu\text{m}$  ( $\approx 1L_n$ ) diameter pillar array, and 32  $\mu\text{m}$  ( $\approx 3L_n$ ) diameter pillar array**

**Table 2 Photovoltaic performance under AM 1.5G illumination of different diameter pillar arrays that have a minority carrier diffusion length of  $L_n \approx 10 \mu\text{m}$**

	n	$J_{\text{dark}}$ (A/cm <sup>2</sup> )	$J_{\text{sc}}$ (mA/cm <sup>2</sup> )	$V_{\text{oc}}$ (V)	FF (%)	efficiency (%)
planar	1.1	$3.3 \times 10^{-12}$	9.6	0.592	80.8	4.6
8 $\mu\text{m}$	1.5	$9.2 \times 10^{-10}$	20.0	0.555	78.1	8.7
32 $\mu\text{m}$	1.3	$1.1 \times 10^{-10}$	10.7	0.573	79.0	4.8

## SUMMARY

In summary, radial junction micropillar arrays based on p<sup>+</sup> crystalline Si substrates ( $5 \times 10^{18} \text{ cm}^{-3}$ ) with a short minority carrier diffusion length ( $L_n \approx 10 \mu\text{m}$ ) were fabricated in different cell geometries. The PV properties of the pillar arrays were analyzed to gain insight into the design tradeoffs. The largest improvement in the efficiency of the pillar array cells is due to the higher values of  $J_{\text{sc}}$ , while the values of  $V_{\text{oc}}$  and FF that are comparable to all cell geometries. These results demonstrate that the radial junction pillar array architecture is effective for enhancing the conversion efficiency of solar cells fabricated using cost-effective materials and fabrication processes.

## ACKNOWLEDGEMENT

This work was supported by US Department of Energy under Contract #DE-PS36-07GO97025 and the use of facilities at the Penn State Site of the NSF NNIN under Agreement #0335765. H.P.Yoon thanks UMD/NIST for financial travel support.

## REFERENCES

- [1] M. Kayes, H. A. Atwater, and N. S. Lewis, "Comparison of the device physics principles of planar and radial p-n junction nanorod solar cells", J. Appl. Phys. 97, 114302 (2005)
- [2] Z. Fan, et al., "Challenges and prospects of nanopillar-based solar cells", Nano Res. 2, 829 (2009)
- [3] Garnett, E.; Yang, P. D, "Light Trapping in Silicon Nanowire Solar Cells", Nano. Lett. 10, 1082 (2010)
- [4] H. Yoon, et al., "Enhanced conversion efficiencies for pillar array solar cells fabricated from silicon with short minority carrier diffusion lengths", Appl. Phys. Lett. 96, 213503 (2010)
- [5] D. Kim, et al., "Hybrid Si Microwire and Planar Solar Cells: Passivation and Characterization", Nano. Lett. (web) May 24 (2011)

[6] Z. Fan, et al., "Three-dimensional nanopillar-array photovoltaics on low-cost and flexible substrates", *Nat. Mater* 8, 648 (2009)

[7] B. Kayes, et al., "Comparison of the device physics principles of planar and radial p-n junction nanorod solar cells", *J. Appl. Phys.* 97, 114302 (2005)

[8] E. Kosten, et al., "Ray optical light trapping in silicon microwires: exceeding the  $2n^2$  intensity limit", *Optics Express* 19, 3316 (2011)

[9] M. Tyagi and R. Vanoverstraeten, "Minority carrier recombination in heavily-doped silicon," *Solid-State Electron.* 26, 577 (1983)